Colloids and Surfaces B: Biointerfaces 169 (2018) 168–175

Contents lists available at ScienceDirect

Colloids and Surfaces B: Biointerfaces

journal homepage: www.elsevier.com/locate/colsurfb

Graphene-kaolin composite sponge for rapid and riskless hemostasis

Yuping Liang[a], Congcong Xu[a], Guofeng Li[a], Tianchi Liu[b], Jun F. Liang[b], Xing Wang[a,b,*]

[a] Beijing Laboratory of Biomedical Materials, Beijing University of Chemical Technology, Beijing 100029, PR China
[b] Department of Biomedical Engineering, Chemistry, and Biological Sciences, Charles V. Schaefer School of Engineering and Sciences, Stevens Institute of Technology, Hoboken, NJ 07030, USA

ARTICLE INFO

Article history:
Received 28 November 2017
Received in revised form 5 May 2018
Accepted 7 May 2018
Available online 8 May 2018

Keywords:
Graphene
Kaolin
Composite
Sponge
Hemostasis
Trauma

ABSTRACT

Kaolin is an effective and safe hemostatic agent for hemostasis. However, its ontic powder is difficult to use in actual practice. To develop a wieldy and powerful hemostat, composite strategy is usually a good choice. Herein, we developed a graphene-kaolin composite sponge (GKCS), synthesized with graphene oxide sheets, linker molecules and kaolin powders through a facile hydrothermal reaction. SEM observations support that GKCS has a porous structure, and EDS mapping further confirms that kaolin powders are embedded in graphene sheets. Once GKCS is exposed to bleeding, plasma is quickly absorbed inside the sponge, meanwhile blood cells are gathered at the interface. The gathered blood cells are in favor of accelerating clotting due to multi stimulations, including concentration, surface charge and activation of hemostatic factors, originating from both kaolin powders and graphene sponge. As a result, GKCS could stop bleeding in approximately 73 s in rabbit artery injury test. Besides, cytotoxicity and hemolysis assessments highlight that GKCS has a good biocompatibility. These remarkable properties suggest that GKCS is a potential riskless hemostatic agent for trauma treatment.

1. Introduction

Hemorrhage is the leading cause of death in emergency and intraoperative bleeding, which results in complications such as hemorrhagic shock, infection, and organ failures [1–3]. Excessive bleeding causes nearly 40% of deaths and is the main reason of traumatic death [4,5]. Therefore, using safe and efficient hemostatic materials are important to save life. Up to now, many kinds of hemostatic materials have been developed, such as zeolite [6], porous silica [7], granulose [8] and chitosan [9]. For inorganic micro- or meso-porous materials, they promote hemostasis on the base of fast liquid absorption and the enrichment of bloods cells and platelets [10–13]. While organic glyco-based materials prefer to gather red blood cells to accelerate blood clotting by electrostatic interaction and gelation. However, most of those hemostats tend to entrap themselves in scab when exerting their performance, which will weaken hemostatic efficiency and cause unnecessary discomfort.

Recently, our group developed a cross–linked graphene sponge (CGS) acting as hemostatic material, which displays remarkable liquid adsorption capacity, thus resulting in a rapid hemostasis within 4 min [14]. Because of its good biocompatibility, this kind of graphene-based sponge is proved to be a platform to load different kinds of hemostatic materials [15–17]. Changing the cross linker from ethanediamine (EDA) to diaminopropionic acid could improve approximate half minutes for hemostatic performance [15], while the CGS combined with thrombin would stop bleeding within 100 s [16]. Recently, we used the CGS to anchor montmorillonite (MMT), the obtained graphene/MMT composite sponge (GMCS) presented remarkable characteristic, which effectively stopped bleeding in approximately 85 s in rabbit artery injury test [17]. Although GMCS eliminates the side effects of MMT, it is still a psychological disorder that the Food and Drug Administration has limited the usage of MMT as commercial hemostatic products since 2007 due to the risk of thrombosis via blood contact. Therefore, on the basis of those above-mentioned achievements and the demand of risk-free hemostasis, we try to develop a more appropriate agent with higher biosafety.

Kaolin is a natural aluminosilicate mineral [18–20]. It is well known for its remarkable ability to induce and accelerate blood clotting. Since 1950s, kaolin has been used as activating agent for clotting in medical doctor routinely performances. Up to now, kaolin still acts as ingredient for operation hemostasis [20,21]. The formed blood clots could effectively trap kaolin particles in the site of the injury, no risk of wandering their going deep into the body. In particular, in April 2008 the US naval medical research institute announced the successful introduce kaolin into ordinary gauze, which is one choice of hemostats for all branches of the US military [22]. As reported, kaolin could activate Factor XII and platelets

* Corresponding author at: Beijing Laboratory of Biomedical Materials, Beijing University of Chemical Technology, Beijing 100029, PR China.
E-mail address: wangxing@mail.buct.edu.cn (X. Wang).

https://doi.org/10.1016/j.colsurfb.2018.05.016
0927-7765/

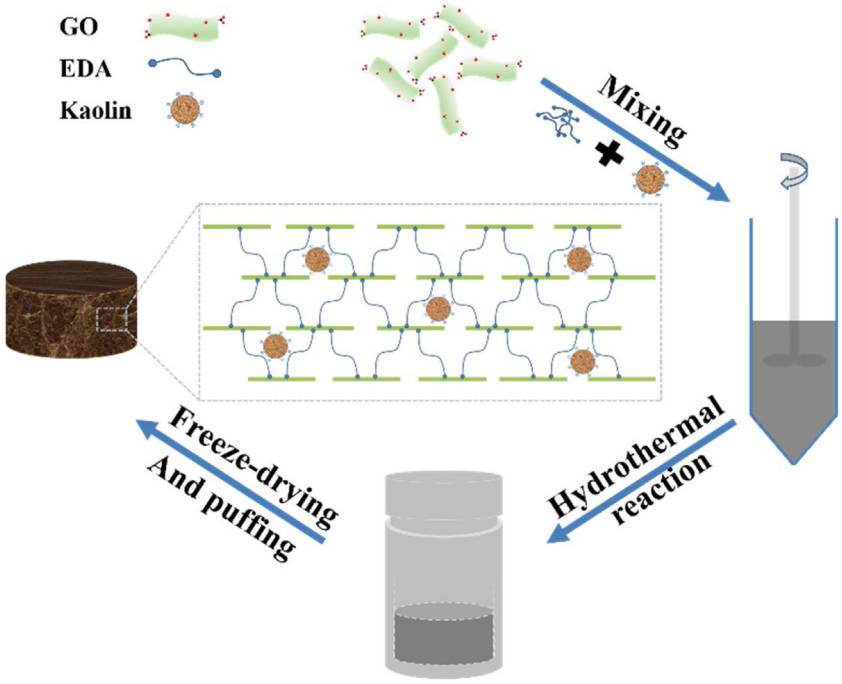

Scheme 1. Schematic representation of the preparation process of GKCS. GO sheets, EDA linkers and kaolin powders are employed to synthesize a hydrogel by a classical hydrothermal reaction. Freeze-drying and puffing are applied to the hydrogel to obtain the final composite sponge, where kaolin powders are fixed in cross-linked GO sheets.

to start the clotting cascade in vivo [20,23,24]. More importantly, kaolin has a good biocompatibility [25]. These outstanding properties highlight that kaolin is a valuable alternative substance.

Herein, we present a graphene-kaolin composite sponge (GKCS), which is synthesized by a facile hydrothermal reaction with graphene oxide (GO) sheets, EDA and kaolin powders (Scheme 1). GO and EDA mainly form the sponge framework, while kaolin powders will be embedded in to act as a new stimulation. GKCS will inherit remarkable liquid absorption capacity due to the porous structure inside, which is the key feature for this graphene-based hemostatic sponge. It can be expected that embedded kaolin into GKCS could improve its hemostatic performance especially with a risk-free way. GKCS is a new step to pursue excellence in traumatic hemostasis, on the platform of graphene-based materials.

2. Materials and methods

2.1. Materials

Graphite powders (80 mesh) were obtained from Qingdao Jinrilai Co., Ltd., Shandong, China. Sulfuric acid (H_2SO_4, 98%), sodium nitrate ($NaNO_3$, AR), potassium permanganate ($KMnO_4$, 99.9%), hydrogen peroxide (H_2O_2, 30%) and hydrochloric acid (HCl, 37%) were obtained from Sigma-Aldrich Co. The GO solution was prepared with improved Hummers' method [26], and the density of GO solution came to 7.5 mg mL^{-1}. The kaolin powders were purchased from Huawei Co., Ltd. (Beijing, China).

2.2. Preparation and characterization of GKCS

Kaolin powders (60 mg) were mixed with 60 mL of GO solution by a high-speed blender. After that, 0.9 mL of EDA was added to the mixture, new mixture needed to be mixed for the second time at the same condition. The mixed solution was sealed in a hydrothermal synthesis reaction kettle, which was heated to 96 °C and set for 6 h to get a hydrogel. The hydrogel was frozen at −4 °C for 2 h and moved into a freeze-dried machine for 2 days. Then the dry hydrogel was fed in Soxhlet extractor with ethanol for 2 days. After drying again, 5 s puffing was applied to obtain the final composite sponge. Changing the addition amount of kaolin powders from 1 mg mL^{-1} to 2, and 5 mg mL^{-1} in GO solution, different composite sponges (the ratio of kaolin/GO = 1:1, 2:1 and 5:1, w/v) were prepared with the above-mentioned method.

Scanning electron microscopy (SEM, 7800) was employed to observe the inside structure of GKCS. Energy-dispersive spectrometry (EDS, Hitachi S-4700) was employed to analyze the surface element content of GKCS. Fourier transform infrared (FT-IR) spectra of pure GO, kaolin and GKCS were recorded over a wave number range of 4000–990 cm^{-1}. Thermogravimetric analysis (TGA, Mettler Toledo TGA/DSC1/1100SF) was used to analyze the kaolin powders content of the GKCS. Zeta potential (Malvern NanoSizer ZS 2000) was employed to assess the negative potential value of GKCS and kaolin powders. Brunauer–Emmet–Teller (BET) surface area measurements were determined by the nitrogen gas adsorption method by using a Micromeritics ASAP 2460 2.02 analyzer at liquid nitrogen temperature.

The liquid absorption of GKCS was assessed by utilizing a CGS control. The absorption capability was measured by weighting GKCS on the condition of absorbing liquid or not. In addition, the absorption rate was scaled by recording the time that a liquid drop got into materials.

2.3. Assessment of the hemostatic performance

The hemostatic performance of GKCS was evaluated with the rabbit femoral artery injury model. NEW Zealand rabbits (weight 2.0–2.5 kg, n = 3) were obtained from Beijing Fuhao Experimental Animal Breeding Center (Beijing, China). Experimental animal treatment was carried out as reported [16]. After the femoral artery was transected, the blood loss at first 30 s was recorded to make sure all of experimental animal in same condition. Then, a piece of GKCS (4 cm diameter, 2 cm thickness) was slight compressed on the wound. The GKCS was slightly uplifted every 10 s to observe if the gap stop bleeding or not. When the gap stopped bleeding, the time and blood loss was recorded. After that, sufficient physiolog-

ical saline was employed to clean the wound, and the wound was sutured later.

2.4. Hemolysis assay in vitro

The anticoagulated blood was obtained from SD rats. The treatment was carried out as reported to obtain the RBCs. To assess the hemolytic activity of materials, 0.2 mL of diluted RBCs was added into 0.8 mL of the sample's suspension solutions in PBS at several concentrations (from 15.6 to 1000 $\mu g\,mL^{-1}$). To get the sample's solutions, added sample's powders in PBS and treated with sonication for 2 h. PBS (+RBCs) and Deionized water (+RBCs) were chosen as negative and positive controls. These samples were put into a rocking shaker for 3 h at 37 °C. After that, these samples were centrifuged at 10,000 *g* for 5 min. The absorbance value of samples' solution was measured with a UV–vis spectrophotometer at 540 nm. The hemolysis rate was calculated by the following formula:

$$\text{hemolysis}\ (\%) = \frac{\text{Abs}_{\text{sample}} - \text{Abs}_{\text{negative}}}{\text{Abs}_{\text{positive}} - \text{Abs}_{\text{negative}}} \times 100\%,$$

where Abs_{sample}, $Abs_{negative}$ and $Abs_{positive}$ corresponded to the absorbance of the samples, negative control and positive control, respectively.

2.5. Cytotoxicity assay

L929 (rat's fibroblast cells, obtained from Cell Resource Center, IBMS, CAMS/PUMC, Beijing, China) was adjusted to 5×10^4 cells mL^{-1} in complete medium (CM), which consisted of 90% RPMI-1640 medium, 10% fetal bovine serum (FBS), and 1% antibiotics (100 units mL^{-1} penicillin and 100 units mL^{-1} streptomycin). The cells suspension was added to 6-well plates (2 mL for each well) and cultivated for 12 h at 37 °C (5% CO_2). Then the materials' suspensions (the solvent is complete medium) were added to 6-well plates after the original medium got removed. The plates were cultivated for 24 h after that PBS was employed to wash cells twice, and these cells were observed under electron microscope; the cell concentration of L929 was calculated with a hemocytometer.

Total RNA was extracted from L929 cells using Tri–Reagent (Molecular Research Center, Inc., Cincinnati, OH). Quantitative real–time PCR was performed using the Power SYBR Green PCR Master Mix protocol (Applied Biosystems, Foster City, CA). Amplification of β–actin was used as an internal reference. Quantitative PCR analysis was conducted using the ABI 7500 Sequence Detection System.

3. Results and discussion

3.1. Material characterization

The prepared GKCS was a black and lightweight sponge (Fig. 1A; 4 cm diameter, 2 cm thickness). Even through kaolin powders were added, the obtained sponge completely inherits apparent property of CGS [14]. As Fig. 1B shows, there are many cross-linked layers inside of the GKCS, which macroscopically build the loose structure of GKCS. Observations under SEM showed that there is thousands of microlayers crisscross to form a porous structure inside of GKCS (Fig. 1C). According to an enlarged image of Fig. 1C, we can find out that one microlayer in Fig. 1C consists of a large number of folded thinner layers (Fig. 1D). These images proved that GKCS perfectly inherit the porous structure of CGS. Consider that porous structure bonds to good adsorption performance, it is reasonable to expect

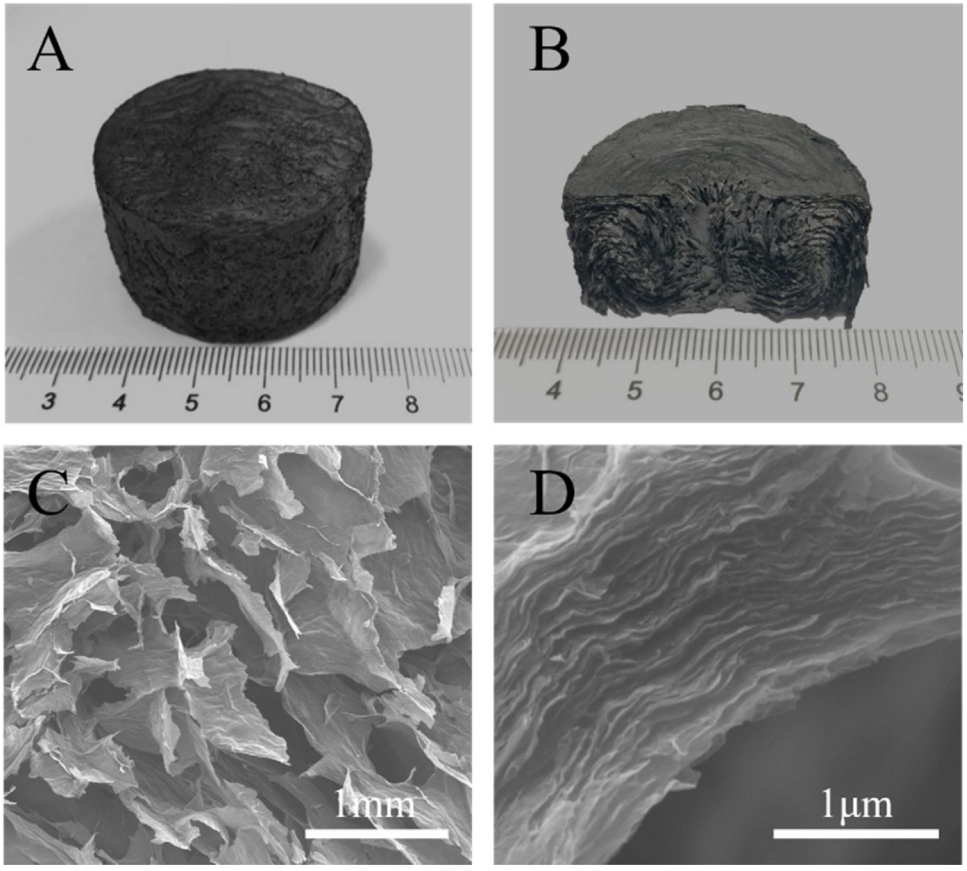

Fig. 1. (A) Photograph of the GKCS; (B) Section of the GKCS; (C) SEM image of the porous structure of the GKCS; (D) The lamellar structure of GKCS.

that GKCS has good liquid absorption ability. This will be discussed in details later.

SEM and EDS were employed to evaluate the distribution of kaolin powders within GKCS. Fig. 2A and B present that kaolin powders are anchored into graphene sheets. According to the enlarged image of sample surface (Fig. 2A' and B'), the size of kaolin powders ranges from 2 to 4 μm. Besides, Zetasizer was used to check out the statistic size of kaolin powders, and the results indicated the size of used kaolin powders consist of 1357 nm (intensity 49.6%) and 4304 nm (intensity 50.4%). The average particle size of kaolin powders is 2353 nm, which is agreed to the SEM and TEM measurements (Fig. 1S). Then, EDS mapping was performed to confirm that kaolin powders are embedded into graphene sheets (Fig. 2B1–B4). Fig. 2B1 and B2 exhibits the uniform C and N elements with different density respectively, which are mainly contributed by EDA-cross-linked graphene sheets. Fig. 2B3 and B4 shows the dispersed Al and Si elements, respectively, which are the characteristic constituents of kaolin powder. These EDS mapping results further confirmed that kaolin powders have effectively composited into CGS. Meanwhile, the results of TGA supported that the GKCS contained about 9.94% (w/w) Kaolin powders (Fig. S2).

FT–IR spectra (Fig. 3) further proved the linkage between GO and EDA. After the reduction of GO with EDA (also see XRD measurements in Fig. 3S), there is a dramatic decrease in the intensities of the peaks corresponding to the oxygen functionalities, such as the —OH deformation vibration peaks (3218 cm^{-1} and 1418 cm^{-1}).

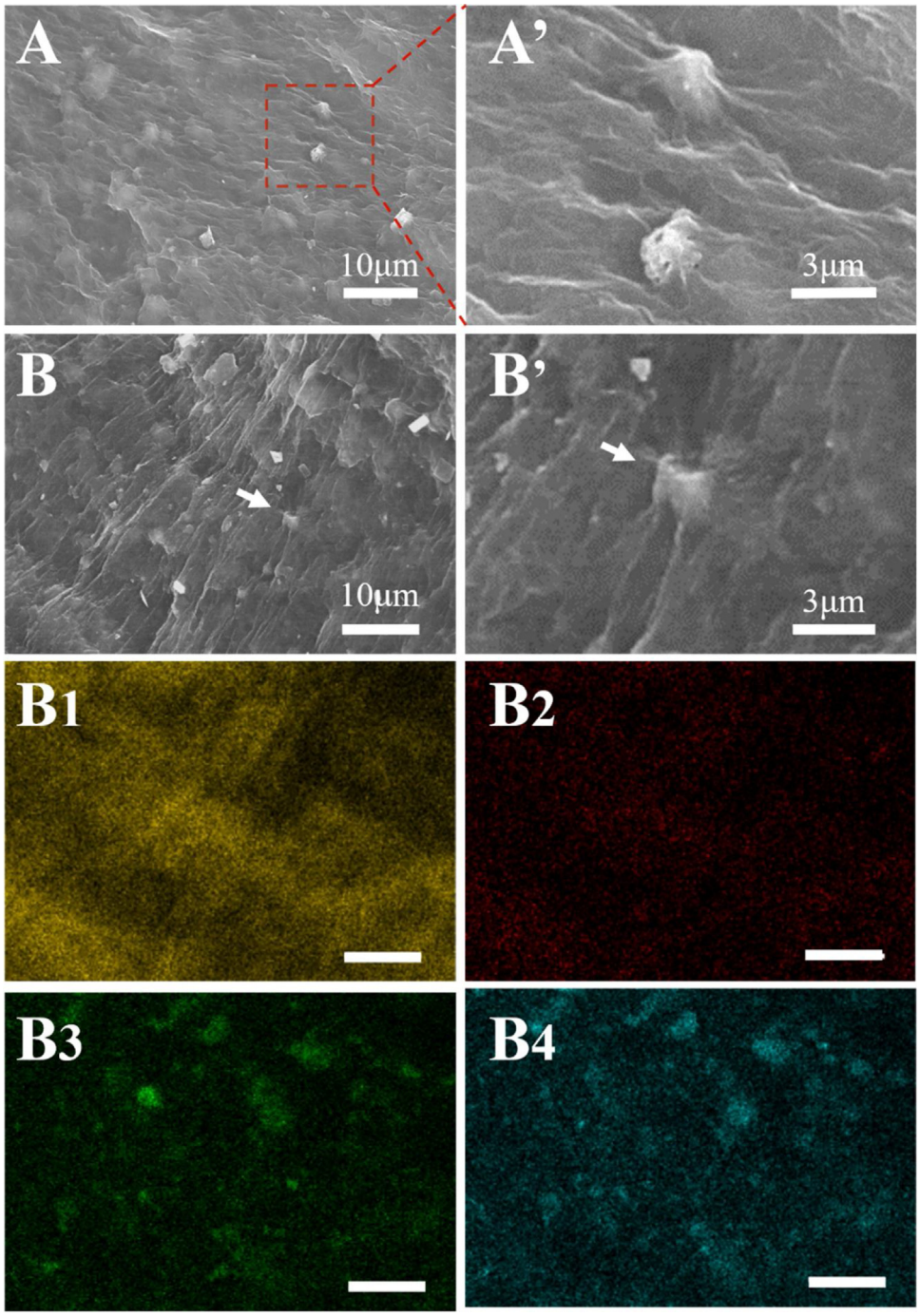

Fig. 2. (A) SEM image of the GKCS surface; (A') The enlarged image from A; (B) EDS micro image of GKCS; (B') The enlarged part of image B; (B1-B4) The EDS mapping of image B indicating C, N, Al and Si elements, respectively.

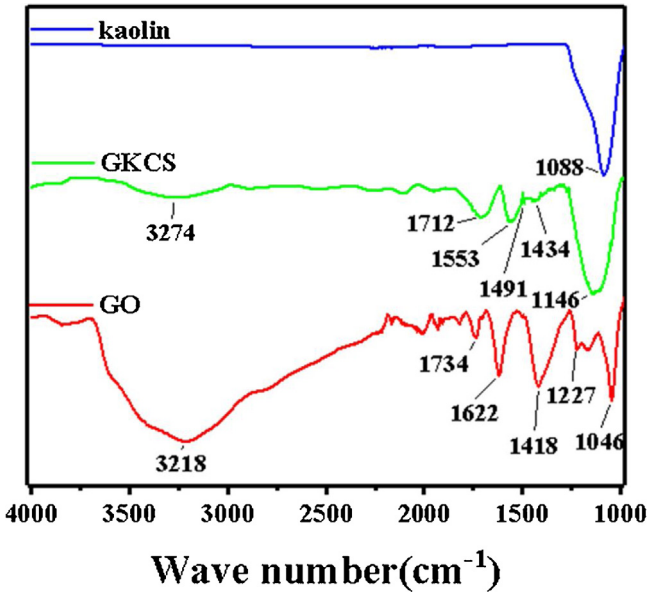

Fig. 3. FT-IR spectra of Kaolin, GO and GKCS.

The intensity of the epoxy and alkoxy peaks at 1224 cm^{-1} and 1060 cm^{-1} also decreases in GKCS. The appearance of new peaks in the region of 1553 cm^{-1} is attributed to the presence of strong in–plane C—N scissoring absorptions [27]. Low intensity or shoulder bands appearing in these spectra in the 1465–1400 cm^{-1} region are due to the antisymmetric C—N stretching vibrations coupled with the out–of–plane NH_2 and NH modes [28]. The strong absorption at 3274 cm^{-1}, 1712 cm^{-1}, and 1146 cm^{-1} can be associated with N—H, C=O and Si—O. Those changes of functional groups confirmed that GKCS is cross-linked successfully.

GKCS perfectly inherited the porous structure of CGS. Therefore, GKCS has a remarkable liquid absorption capability. Fig. 4A presents that GKCS can absorb a water droplet within 40 ms (for blood, the value comes to 80 ms). This rate indicates the composite sponge a remarkable capability of liquid absorption. Increasing the dose of kaolin (the ratio of kaolin/GO from 1:1 to 5:1, w/v) would weaken the absorption capacity of the composites (Fig. S4), which would decrease their hemostatic performance [17]. The GKCS (1:1, w/v) possessed the best absorption capacity, and therefore, it was further investigated. As to liquid absorption capacity (Fig. 4B), the water absorption amount of GKCS is 706.2 ± 44.0 mg mL^{-1}. Compared with CGS (955.4 ± 59.0 mg mL^{-1}), kaolin powders occupy part of the interior space of GKCS will be the reason for the decrease. While for blood, the amount of GKCS is 639.1 ± 2.5 mg mL^{-1}, much lower than that of CGS (1226.7 ± 35.4 mg mL^{-1}). Kaolin powders embedded in GKCS are the reason. In some way, GKCS promotes blood clotting that prevents blood from getting inside of this sponge. This interesting phenomenon also hinted the powerful performance of hemostatic GKCS.

As reported previously, to promote performance of hemostatic materials, two points need to be noted: fast absorbing liquid to enrich blood cells and speedup activation of blood factors [29,30]. It has been confirmed that potentials are one of stimulations. As a mineral, kaolin powders get negative charge on surface [31,32]. Its potential value comes to -35.46 ± 0.68 mV (Fig. 4C). Due to existing of polar functional groups such as hydroxyl and carboxyl groups, CGS gets a negative potential as well; the potential value is -19.9 ± 2.1 mV for CGS. After combining these two substances, as Fig. 4C presents, the negative potential value of GKCS comes to -22.08 ± 2.50 mV. It means that GKCS would have a stronger stimulate for blood cells than CGS to accelerate clotting. Though the potential of composite is lower than that of naked kaolin, GKCS changes the blood distribution from kaolin-in-scab to kaolin-out-scab, which will continue producing irritation. It is significant for both kaolin powders and CGS to improve their hemostatic performance.

Fig. 4D shows the N_2 adsorption–desorption isotherm of GKCS. According to IUPAC classification, the curve is characterized by type IV with a H_2 hysteresis loop at a relative pressure P/Po ranging from 0 to 1.0, which indicates the regular size and shape of pores exists in GKCS. As a result, a single peak was found in the analysis of BJH pore size distribution (Fig. 4E). Based on the data of N_2 adsorption–desorption isotherm of GKCS, the calculated BET surface area of GKCS comes to be 47.64 ± 0.26 m^2 g^{-1}, and the BJH adsorption average pore diameter (4 V A^{-1}) is 4.15 nm. These data indicate that GKCS owns the similar specific surface area compared

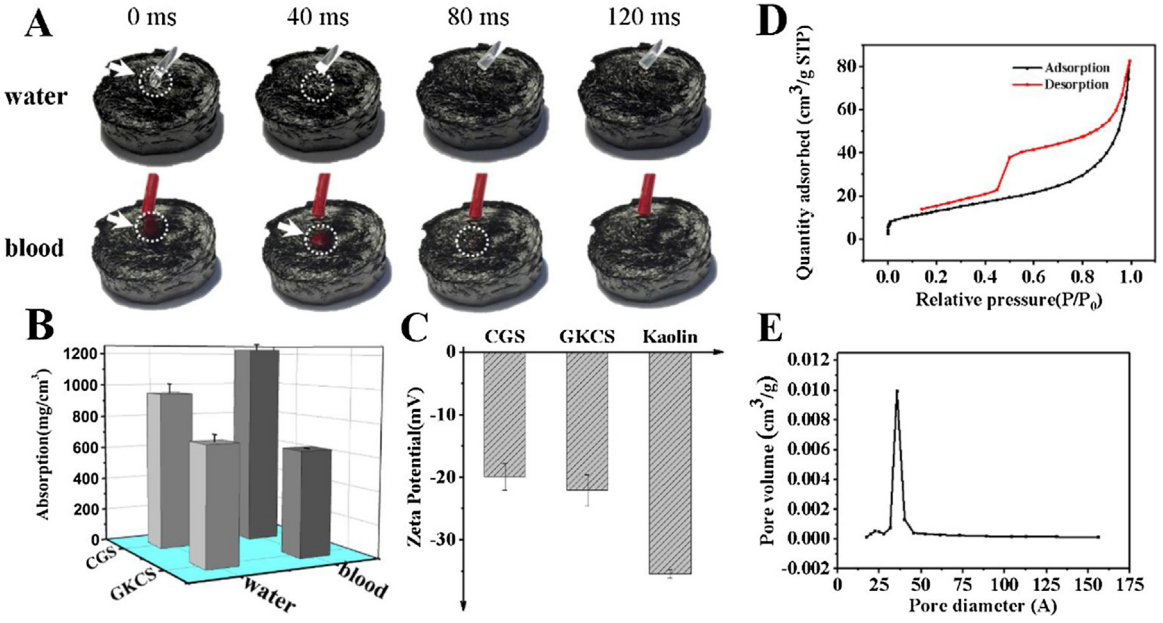

Fig. 4. (A) The liquid absorption rate of GKCS; (B) The liquid absorption amount of CGS, and GKCS; (C) The zeta potential of CGS, GKCS, and Kaolin; (D) The N_2 adsorption–desorption isotherm of GKCS; (E) The BJH pore size distribution of GKCS.

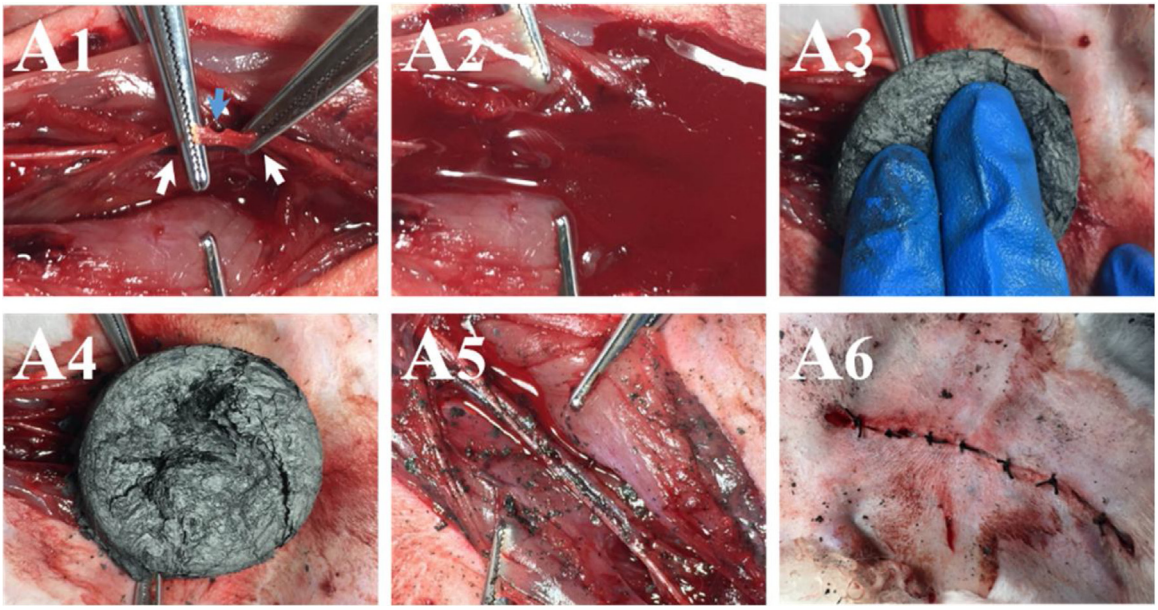

Fig. 5. (A) Hemostatic evaluation of GKCS by using rabbit artery injury model; (A1) Isolated arteries and create damage in the artery; (A2) Bleeding from the wound; (A3) GKCS was exposed to wound; (A4) Hemostasis was completed; (A5) The wound after removing the material; (A6) Stitched wound.

with basic CGS ($42.9 \pm 1.9\ m^2\ g^{-1}$) [14], thus expecting a more powerful hemostatic property.

3.2. Hemostatic performance

Evaluation of hemostatic performance was carried out in rabbit artery injury model (Fig. 5A). New Zealand rabbits (weight 2.0–2.5 kg) were used as the experimental animals (n = 3). At first, the artery was isolated from surrounding tissues, and half damage was created at the artery (Fig. 5A1, the wound is marked with blue arrow). Once the artery bleeding started, recorded the blood loss in 30 s to make sure all of animals under the same condition (Fig. 5A2, a total of 7.2 ± 3.1 mL). Then the wound was exposed to GKCS, under the operation pressure (Fig. 5A3), blood was quickly absorbed (Fig. 5A4) and the wound got cured in approximate 73 ± 12 s (Fig. 5A5). At last, the wound was stitched (Fig. 5A6). Based on this treatment, all experimental rabbits were recurred. After one week, the operative legs recovered normal motor function, and the mortality rate of the rabbits was 0%.

These results demonstrated that GKCS is a valuable material for hemostasis. GKCS perfectly inherited porous structure of graphene-based sponge. Porous structure endows GKCS sufficient vacuum and good liquid absorbency and retention. Within GKCS, kaolin is anchored into graphene layers. When GKCS is exposed to bleeding wound (Scheme 2), plasma is adsorbed into GKCS quickly. On one hand, blood cells enrich on the surface of GKCS, accelerating blood clotting as normal absorb agent [14,15]; on the other hand, once plasma touches with kaolin powders, Factor XII and platelets will be activated soon [33]. Factor XII is a serine protease zymogen, which will get activated by negative potential and change to Factor XIIa. Factor XIIa is formed and triggers the intrinsic pathway of blood coagulation (Scheme 2 inset). Besides, with the presence of activated platelets, Factor XIa bonds to Factor VIII to form intrinsic tenase which will efficiently activate Factor X. Factor Xa then binds to Factor Va to form prothrombinase, thereby increasing the resultant burst of thrombin (Factor IIa) > 300 000-fold, and rapidly converts fibrinogen (Factor I) to fibrin (Factor Ia) thus promoting cross-linked polymerization of fibrin to form blood clotting [33].

3.3. Hemolysis assay in vitro

Hemolysis test was carried out to assess the biocompatibility of GKCS. According to our experiments (Fig. 6A), the kaolin-dispersed solution presents a transparency as same as the negative control. The dose changes of kaolin have almost no effect on it (Fig. 6A), though increasing dosage will induce a slight higher hemolysis (Fig. 6B), where the max rate is no more than 2%. It means kaolin has little toxic to blood cells. This result is also agreed with previous study [34]. For GKCS, no hemolysis risk (below 5%, the green line in Fig. 6B) was found as well as kaolin powders (Fig. 6). On the base

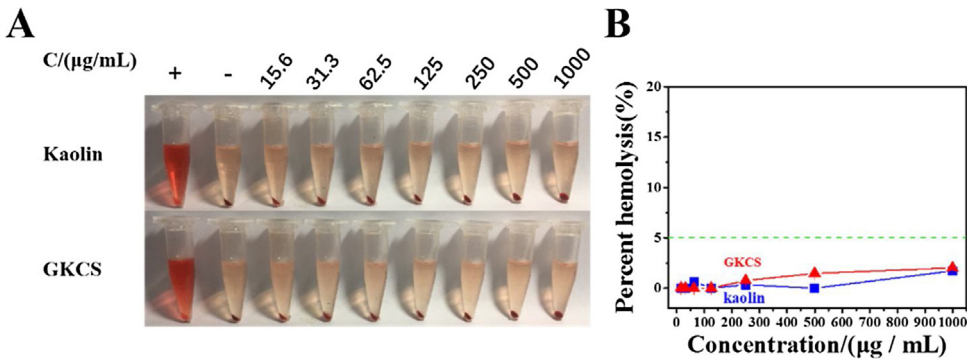

Fig. 6. (A) The results of hemolysis assays for kaolin powders and GKCS; (B) Hemolysis rate of kaolin and GKCS, 5% is the minimum concentration required for the occurrence of hemolysis (the green dotted line of B). (For interpretation of the references to colour in this figure legend, the reader is referred to the web version of this article.)

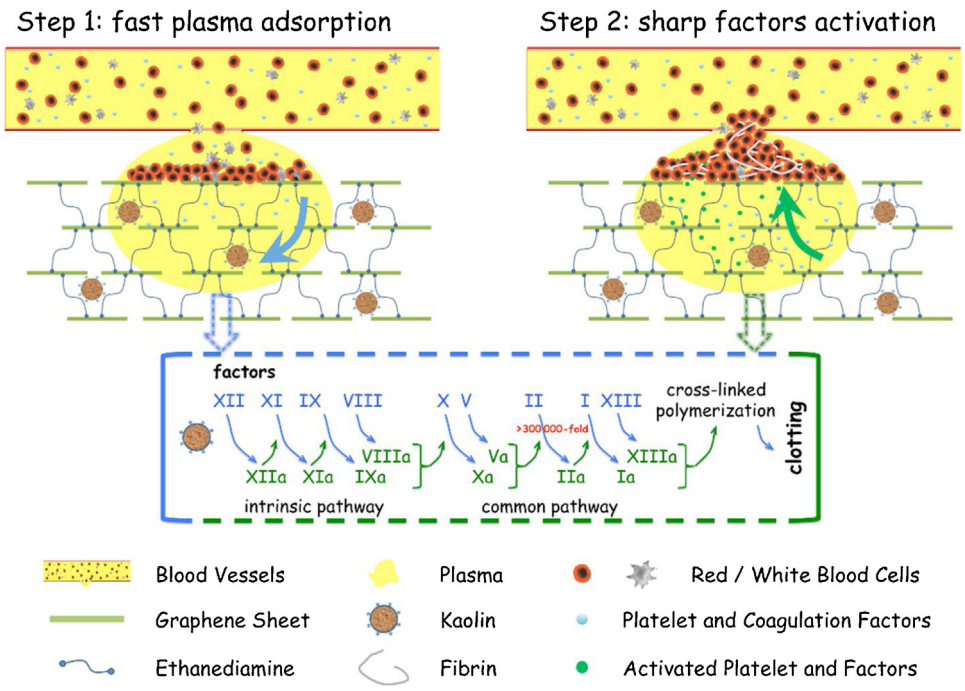

Scheme 2. Schematic representation of the hemostatic mechanism for GKCS. First step is fast plasma adsorption based on CGS property; second step is sharp coagulation factors and platelet activation mainly based on kaolin powders' stimulation. Inset shows the most Factors involved in clotting process, such as Factor II (prothrombin), Factor IIa (thrombin), Factor I (fibrinogen), and Factor Ia (fibrin).

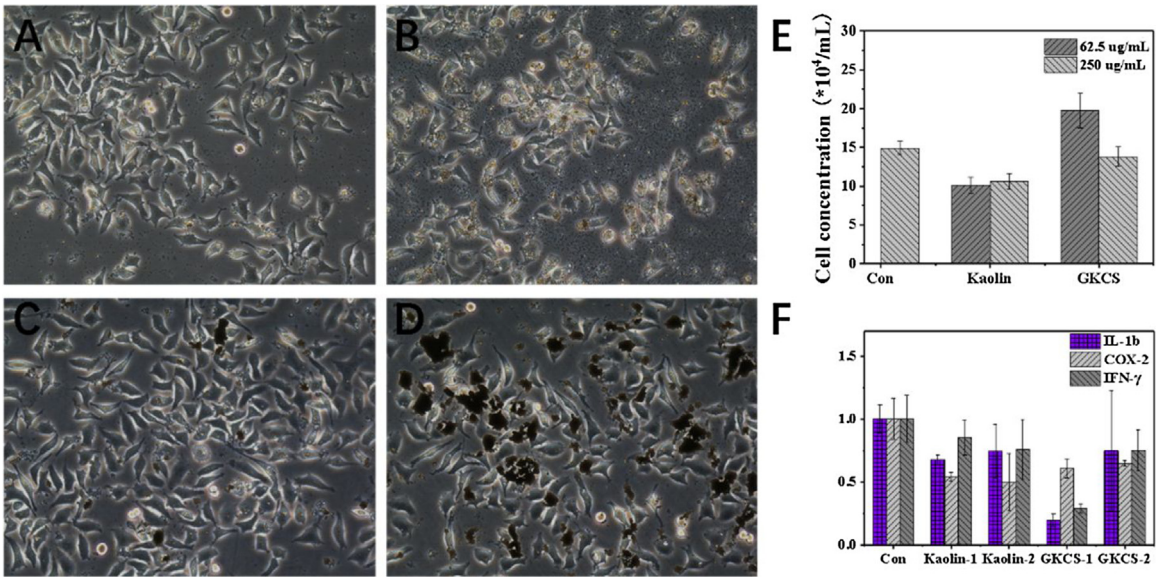

Fig. 7. L929 cells cultured with kaolin treatments (A, B) and GKCS treatments (C, D). (A, C) Dosage is 62.5 μg mL^{-1}; (B, D) dosage is 250 μg mL^{-1}. (E) The statistic cell concentration of A–D. (F) The gene expression level of IL–1, NF–kB (COX–2, IFN–γ) for A (kaolin–1), B (kaolin–2), C (GKCS–1), and D (GKCS–2).

of the above phenomena, it is safe for both kaolin and GKCS to be used as blood contact product. In other words, GKCS have a good biocompatibility with blood cells.

3.4. Cytotoxicity assessment

The cytotoxicity of hemostatic materials is also an important factor. Kaolin has been used as ingredient for operation hemostasis for many years [20,21]. For example, nonwoven gauze impregnated with kaolin (QuikClot Combat Gauze) has used as one of hemostat for the US military [22]. It has also been reported that graphene has a good biocompatibility to cells [35]. For their complex, according to the reports [36], L929 cells were chose to assess the cells compatibility of GKCS. Fig. 7 shows the morphologies of the tested L929 cells. Cells maintain a normal form (Fig. 7A) when lower dosage of kaolin (62.5 μg mL^{-1}) was co-cultured. However, when the cells were cultured with higher dosage of kaolin (250 μg mL^{-1}), the form of partial L929 cells changed to oval morphologies (Fig. 7B). While for GKCS co-cultured with the same dosage, no distinct changing was observed (Fig. 7C and D), or the dose changes did not have an obvious effect on cell morphologies. Meanwhile, Fig. 7E shows the statistic cell concentration of above-mentioned observation. The result indicates that GKCS has better biocompatibility than kaolin, demonstrating GKCS's potential for use in traumatic hemostasis.

It has been reported that compared with standard gauze, kaolin–impregnated gauze could inhibit the production of inflam-

mation during surgery [19]. Fig. 7F shows that this GKCS inhibits the expression of inflammatory genes in a concentration–dependent manner, especially for IL–1 and IFN–γ. Lower dosage of GKCS (62.5 μg mL^{-1}) triggers lower inflammatory gene expression level. It is in accord with that lower dosage of GKCS group has higher cell concentration (Fig. 7E), where the rapid growth of cells may result into lower inflammatory gene expression. Anyway, compared with control group, all those four groups of kaolin powders and GKCS samples exhibit inhibiting effect on the inflammatory genes expression including IL–1, COX–2 and IFN–γ. Consider the feature of GKCS for using in trauma treatment, it is riskless from both tissue and blood slant.

Nowadays, some researchers worry about nano materials that are potentially toxic to human body. Although researchers have raised concerns about the safety of nanoparticles, free kaolin powders have been used on human body [19–22]. In addition, by triggering blood clotting, these particles effectively trap themselves at the site of the injury, demonstrating no thrombus or other risk to human body. While for GKCS, graphene framework has a good biocompatibility and can be used as biomedical materials [14,35]. By perfectly embedding kaolin in graphene sheets, those powders could not get in deep of human body. But at the same time, kaolin powders could still activate factors in plasma to speedup blood clotting. Besides, GKCS is a traumatic hemostatic agent that will be removed after bleeding control. Therefore, GKCS is safe and riskless for trauma patients.

4. Conclusions

In summary, we synthesized a new hemostatic sponge GKCS with graphene sheets and kaolin powders. GKCS could stop bleeding in approximately 73 s in rabbit artery injury model. It has two characteristics to speed blood clotting up. First, GKCS owns a porous structure just like CGS, making it possible to fast absorb liquid and gather blood cells; besides, as an effective hemostatic agent, kaolin was embedded into graphene layers, which will activate hemostatic factors such as Factor XII, Factor X, Factor V and platelets to accelerate hemostasis. In the synergy of fast plasma adsorption and then interfacial stimuli, GKCS made great progress on bleeding control. Not only its efficacy is much better than other CGS-based hemostats, also its safety is guaranteed due to the using of more biocompatible kaolin ingredients. Hemolysis assessment and cytotoxicity evaluation in vitro highlighted that GKCS has a good biocompatibility for both blood system and tissue cells. Compared with naked kaolin powders, GKCS employees less kaolin powders (less than 10^{-6} v/v) but displays remarkable hemostatic performance (three times shorter than kaolin powders that usually stop bleeding after 4 min) with the help of graphene network. While to compare with CGS (stop bleeding within 4 min), GKCS can arouse forceful stimuli at interface, where those powders do not change the construction or main morphology of graphene sponge. Moreover, there is no need to worry about any possible leakage of kaolin powders. Therefore, this effective and riskless composite is far more successful in the field of graphene-based hemostasis.

Acknowledgments

The authors thank the National Natural Science Foundation (21574008), the Fundamental Research Funds for the Central Universities (PYBZ1709, BHYC1705B and XK1701) of China, and National Institute of Health (NIH, AI110924) for their financial support. Dr. Xing Wang also gratefully acknowledges China Scholarship Council for their financial support on a Visiting Scholar Program (No. 201706885008).

Appendix A. Supplementary data

Supplementary data associated with this article can be found, in the online version, at https://doi.org/10.1016/j.colsurfb.2018.05.016.

References

[1] A. Sauaia, F.A. Moore, E.E. Moore, J.B. Haenel, R.A. Read, D.C. Lezotte, Arch. Surg. 129 (1994) 39–45.
[2] N. Cosgriff, E.E. Moore, A. Sauaia, M. Kenny-Moynihan, J.M. Burch, B. Galloway, J. Trauma 42 (1997) 857–862.
[3] S.R. Heckbert, N.B. Vedder, W. Hoffman, R.K. Winn, L.D. Hudson, G.J. Jurkovich, M.K. Copass, J.M. Harlan, C.L. Rice, R.V. Maier, J. Trauma 45 (1998) 545–549.
[4] F. Moore, K. Moser, R. Read, P. Pons, J. Trauma 38 (1995) 185–193.
[5] L.W. Chan, X. Wang, H. Wei, L.D. Pozzo, N.J. White, S.H. Pun, Sci. Transl. Med. 7 (2015), 277ra229–277ra229.
[6] A. Shander, L.J. Kaplan, M.T. Harris, I. Gross, N.P. Nagarsheth, J. Nemeth, S. Ozawa, J.B. Riley, M. Ashton, V.A. Ferraris, J. Am. Coll. Surg. 219 (2014) 570–579.
[7] C.N. Sambasivan, S.D. Cho, K.A. Zink, J.A. Differding, M.A. Schreiber, Am. J. Surg. 197 (2009) 576–580.
[8] F. Chen, X. Cao, J. Yu, H. Su, Q. Gan, H. Hong, C. Liu, Colloids Surf. B 159 (2017) 937–944.
[9] J.R. Bell, Skin Allergy News 38 (2007), 32–32.
[10] N. Ahuja, T.A. Ostomel, P. Rhee, G.D. Stucky, R. Conran, Z. Chen, G.A. Al-Mubarak, G. Velmahos, H.B. Alam, J. Trauma 61 (2006) 1312–1320.
[11] B.G. Kozen, S.J. Kircher, J. Henao, F.S. Godinez, A.S. Johnson, Acad. Emerg. Med. 15 (2008) 74–81.
[12] C. Dai, Y. Yuan, C. Liu, J. Wei, H. Hong, X. Li, X. Pan, Biomaterials 30 (2009) 5364–5375.
[13] C. Dai, C. Liu, J. Wei, H. Hong, Q. Zhao, Biomaterials 31 (2010) 7620–7630.
[14] K. Quan, G. Li, D. Luan, Q. Yuan, L. Tao, X. Wang, Colloids Surf. B 132 (2015) 27–33.
[15] X. Zhang, J. Yin, C. Peng, W. Hu, Z. Zhu, W. Li, C. Fan, Q. Huang, Carbon 49 (2011) 986–995.
[16] K. Quan, G. Li, L. Tao, Q. Xie, Q. Yuan, X. Wang, ACS Appl. Mater. Interfaces 8 (2016) 7666–7673.
[17] G. Li, K. Quan, Y. Liang, T. Li, Q. Yuan, L. Tao, Q. Xie, X. Wang, ACS Appl. Mater. Interfaces 8 (2016) 35071–35080.
[18] W.A. Deer, R.A. Howie, J. Zussman, Rock-forming minerals vol.36, Longmans, London, 1966, pp. 150–151.
[19] M.E. Chávez-Delgado, C.V. Kishi-Sutto, X.N.A.D. La-Riva, M. Rosales-Cortes, P. Gamboa-Sánchez, J. Surg. Res. 192 (2014) 678–685.
[20] M.J. Sena, G. Douglas, T. Gerlach, J.K. Grayson, K.O. Pichakron, D. Zierold, J. Surg. Res. 183 (2013) 704–709.
[21] R. Davies, D. Griffiths, N. Johnson, A. Preece, D. Livingston, Br. J. Exp. Pathol. 65 (1984) 453–466.
[22] Y. Ran, E. Hadad, S. Daher, O. Ganor, J. Kohn, Y. Yegorov, C. Bartal, N.A.G. Hirschhorn, Prehosp. Disaster Med. 25 (2010) 584–588.
[23] M.J. Sena, S. Larson, N. Piovesan, G. Vercruysse, Am. Surg. 76 (2010) 774–775.
[24] F. Arnaud, D. Parreno-Sadalan, T. Tomori, M.G. Delima, K. Teranishi, W. Carr, G. McNamee, A. McKeague, K. Govindaraj, C. Beadling, J. Trauma 67 (2009) 848–855.
[25] F.R. Ahmed, M.H. Shoaib, M. Azhar, S.H. Um, R.I. Yousuf, S. Hashmi, A. Dar, Colloids Surf. B 135 (2015) 50–55.
[26] W. Humers, R. Offeman, J. Am. Chem. Soc. 80 (1958), 1339–1339.
[27] N.H. Kim, T. Kuila, J.H. Lee, J. Mater. Chem. A 1 (2012) 1349–1358.
[28] J.L. Yan, G.J. Chen, J. Cao, W. Yang, B.H. Xie, M.B. Yang, New Carbon Mater. 52 (2012) 370–376.
[29] T.A. Ostomel, Q. Shi, P.K. Stoimenov, G.D. Stucky, Langmuir 23 (2007) 11233–11238.
[30] M.A. Dobrovolskaia, A.K. Patri, J. Simak, J.B. Hall, J. Semberova, S.H.D.P. Lacerda, S.E. McNeil, Mol. Pharm. 9 (2012) 382–393.
[31] S. Levis, P. Deasy, Int. J. Pharm. 243 (2002) 125–134.
[32] Y.H. Hu, X.W. Liu, Miner. Eng. 16 (2003) 1279–1284.
[33] S.M. Bates, J.I. Weitz, Circulation 112 (2005) 53–60.
[34] M.H. Yazer, E.M. Glackin, D.J. Triulzi, L.H. Alarcon, A. Murdock, J. Sperry, Transfusion (Paris) 56 (2016) 596–604.
[35] K.H. Liao, Y.S. Lin, C.W. Macosko, C.L. Haynes, ACS Appl. Mater. Interfaces 3 (2011) 2607–2615.
[36] N.L.G. Souza, M. Munk, H.M. Brandão, L.F.C. De Oliveira, Polym. Plast. Technol. Eng. 56 (2017) 1076–1083.